Available online at www.sciencedirect.com
SCIENCE DIRECT®
Polyhedron 25 (2006) 521–529
POLYHEDRON
www.elsevier.com/locate/poly

Synthesis and characterization of the $[Ni_6Ge_{13}(CO)_5]^{4-}$ and $[Ge_9Ni_2(PPh_3)]^{2-}$ Zintl ion clusters

Emren N. Esenturk, James Fettinger, Bryan Eichhorn *

Department of Chemistry and Biochemistry, University of Maryland, College Park, MD 20742, United States

Received 3 June 2005; accepted 21 July 2005
Available online 31 August 2005

Abstract

Reactions between K_4Ge_9, $Ni(CO)_2(PPh_3)_2$, and 2,2,2-crypt in ethylenediamine solutions give two different products depending on reaction conditions. The $[Ni_6Ge_{13}(CO)_5]^{4-}$ ion (**1**) is formed at low temperatures (~40 °C) and short reaction times whereas the $[Ge_9Ni_2(PPh_3)]^{2-}$ ion (**2**) forms at higher temperatures (~118 °C). Both complexes were isolated as $[K(2,2,2\text{-crypt})]^+$ salts and characterized by single-crystal X-ray diffraction, electrospray mass spectrometry (ESI-MS) and NMR studies (^{13}C and ^{31}P). **1** has a hypo-*closo* cluster electron count (Wades Rules) and adopts an interpenetrating biicosahedral structure with 17 vertices and 2 interstitials, which is unique in transition metal Zintl ion clusters. **2** also has a hypo-*closo* cluster electron count but displays an open, *nido*-like 10-vertex structure with a Ni interstitial. The composition of **2** was established through ESI-MS studies and corrects an earlier report that characterized the cluster as $[Ge_{10}Ni(PPh_3)]^{2-}$ with an interstitial Ge.

Keywords: Polygermanide; Zintl; Icosahedron

1. Introduction

Interest in "ligand-free" transition metal derivatives of Zintl ions has received much attention of late due to their close relationship to nanoparticles and fullercages [1–4], their remarkable molecular and electronic structures [5,6] and their utility in preparing low temperature alloys and intermetallics [7,8]. In particular, group 14 Zintl ions (i.e., Ge_9^{4-}, Sn_9^{4-}, Pb_9^{4-}) react with labile transition metal precursors to give high symmetry clusters that often contain centered transition metals. These include the $[M@Pb_{12}]^{2-}$ and $[M@Pb_{10}]^{2-}$ ions where M = Ni, Pd, Pt [9–11], and the recently reported $[Pd_2@Ge_{18}]^{4-}$ and $[Ni_3@Ge_{18}]^{4-}$ clusters [12,13]. The structures of these clusters depend on both the steric demands of the constituent elements and the cluster electron count. Many have structures similar to the boranes and are predicted by Wades rules [14] whereas others, such as $[Sn_9Pt_2(PPh_3)]^{2-}$, seem to violate Wade's structure prediction principles [15]. The latter complex has 20 cluster electrons with 10 surface vertices, which corresponds to a hypo-*closo* system in a Wade type analysis. The observed structure is not the anticipated closed, deltahedral type but a more open, *nido*-like framework [16] with fewer Sn–Sn contacts that predicted. This structural variance presumably results from the steric demands of the centered Pt atom and the weak nature of the Sn–Sn bonds. For comparison, the closely related $[Sn_9Ni_2(CO)]^{3-}$, which has a smaller Ni interstitial, adopts the expected closo structure in accord with its 21 electron, $2n + 1$ configuration [15].

Our initial studies with group 14 Zintl ions involved the use of ML_n subunits that did not contribute electrons to cluster bonding and were not expected to alter the cluster electron count or Zintl ion precursor framework structure. For example, the 9-vertex, 22-electron *nido*-Sn_9^{4-} complex forms the expected 10-vertex,

* Corresponding author.
E-mail address: eichhorn@umd.edu (B. Eichhorn).

0277-5387/$ - see front matter © 2005 Elsevier Ltd. All rights reserved.
doi:10.1016/j.poly.2005.07.031

22-electron *closo*-$[Sn_9M(CO_3)]^{4-}$ series of complexes (M = Cr, Mo, W) [17]. The first transition metal polygermanide was prepared from the reaction between Ge_9^{4-} and $Ni(CO)_2(PPh_3)_2$ in ethylenediamine solvent. The product was characterized as $[K(2,2,2\text{-crypt})]_2[Ge_9(\mu_{10}\text{-Ge})Ni(PPh_3)]$ on the basis of X-ray analysis and Wade's electron counting principles [18]. By inserting an interstitial Ge instead of an interstitial Ni atom, one achieves a nido electron count that is consistent with the observed *nido*-like structure. With the discovery [15] of the isostructural $[Sn_9Pt_2(PPh_3)]^{2-}$ ion that violates Wades rules, we were prompted to reinvestigate the identity of the $[Ge_9(\mu_{10}\text{-Ge})Ni(PPh_3)]^{2-}$ ion by way of electrospray mass spectrometry (ESI-MS) and a new single-crystal X-ray analysis. During the course of our investigation, we discovered a new type of transition metal Zintl cluster, $[Ge_{13}Ni_6(CO)_5]^{4-}$, that possesses an interpenetrating biicosahedral structure [19,20]. Herein we report the synthesis and characterization of this cluster in addition to the correct structure and composition of the $[Ge_9Ni_2(PPh_3)]^{2-}$ ion that was previously described [18] as the $[Ge_9(\mu_{10}\text{-Ge})Ni(PPh_3)]^{2-}$ ion. The interconversion of these complexes and their relationships to other transition metal group 14 Zintl complexes are described.

2. Experimental

2.1. General data

All reactions were performed in a nitrogen atmosphere drybox (Vacuum Atmosphere Co.). The $^{31}P\{^1H\}$ NMR spectrum was recorded on a Bruker DRX400 spectrometer at 162 MHz. Electrospray Mass Spectra (ESI-MS) were obtained by direct injection of DMF solutions into a Finnigan mass spectrometer. Samples were detected in the negative ion mode. An AMRAY 1820K scanning electron microscope with a potential of 20 kV was used for energy dispersive X-ray (EDX) studies.

2.2. Chemicals

Melts of nominal composition K_4Ge_9 was made by fusion (at high temperature) of stoichiometric ratios of the elements. The chemicals were sealed in evacuated, silica tubes and heated carefully with a natural gas/oxygen flame. *CAUTION:* the synthesis of polygermanides can result in explosive mixtures and all fusion reactions should be conducted behind a blast shield inside of a well functioning hood. 4,7,13,16,21,24-Hexaoxa-1,10-diazobicyclo[8,8,8]-hexacosane (2,2,2-crypt) and $Ni(CO)_2(PPh_3)_2$ were purchased from Aldrich. Anhydrous ethylenediamine (en) and dimethylformamide (DMF) were purchased from Fisher, vacuum distilled from K_4Sn_9, and stored under dinitrogen.

2.3. Synthesis

2.3.1. Preparation of $[K(2,2,2\text{-crypt})]_4[Ni_6Ge_{13}(CO)_5]\cdot 1.5en$ (1)

In a vial K_4Ge_9 (54 mg, 0.07 mmol), 2,2,2-crypt (100 mg, 0.27 mmol), and $[Ni(CO)_2(PPh_3)_2]$ (84 mg, 0.14 mmol) were dissolved in 4 ml of en yielding a red/brown mixture. This mixture was heated ($35\ ^\circ C < T < 45\ ^\circ C$) and stirred for about 15 min. and filtered through a hot filter. After a week small thin black crystals of $[K(2,2,2\text{-crypt})]_4[Ni_6Ge_{13}(CO)_5]\cdot 1.5en$ precipitated. Yield: ~20 mg (~30%). EDX Ge:Ni:K = 3.8:1.7:1. ESI-MS data: (*m*/*z*, ion) 1850 $[K(2,2,2\text{-crypt})Ni_6Ge_{13}(CO)_5]^{1-}$; 1821 $[K(2,2,2\text{-crypt})Ni_6Ge_{13}(CO)_4]^{1-}$; 1296 $[Ni_6Ge_{13}]^{1-}$; 1214 $[K(2,2,2\text{-crypt})Ge_9Ni_2(CO)]^{1-}$; 838 $K[Ge_9Ni_2(CO)]^{1-}$; 810 $K[Ge_9Ni_2]^{1-}$; 770 $[Ge_9Ni_2]^{1-}$; 677 $K[Ge_4Ni_4(CO)_4]^{1-}$.

2.3.2. Preparation of $[K(2,2,2\text{-crypt})]_2[Ni_2Ge_9(PPh_3)]\cdot en$ (2)

In a vial K_4Ge_9 (54 mg, 0.007 mmol), 2,2,2-crypt (100 mg, 0.27 mmol), and $[Ni(CO)_2(PPh_3)_2]$ (84 mg, 0.14 mmol) were dissolved in 4 ml of en yielding a red/brown mixture. This mixture was boiled and stirred for about 15 min, and filtered through a hot filter. After 3–4 days block-shaped black crystals of $[K(2,2,2\text{-crypt})]_2[Ni_2Ge_9(PPh_3)]\cdot en$ started to precipitate. Yield: ~20 mg (~30%). EDX analysis on crystals showed presence of K, P, Ge, and Ni. ESI-MS data: (*m*/*z*, ion) 1447 $[K(2,2,2\text{-crypt})Ni_2Ge_9(PPh_3)]^{-1}$, 1072 $K[Ni_2Ge_9(PPh_3)]^{-1}$, 838 $K[Ni_2Ge_9(CO)]^{-1}$, 810 $K[Ni_2Ge_9]^{-1}$.

2.3.3. Interconversion studies

Conversion of ***1*** *to* ***2***. In a dry box, 36 mg of $[K(2,2,2\text{-crypt})]_4[Ni_6Ge_{13}(CO)_5]$ crystals were dissolved in 4 ml DMF. ESI-MS data were recorded to confirm the presence of $[Ni_6Ge_{13}(CO)_5]^-$ and $[K(2,2,2\text{-crypt})][Ni_6Ge_{13}(CO)_5]^-$, $[Ni_2Ge_9(CO)]^-$ and $[Ni_2Ge_9]^-$ ions before the interconversion experiments. 3 mg of PPh_3 was added to the starting solution and the reaction mixture was stirred for 30 min at ~118 °C. The resulting ESI-MS spectra showed signals of $K[Ni_2Ge_9(PPh_3)]^-$ and $[Ni_2Ge_9(PPh_3)]^-$ ions.

Attempted conversion of ***2*** *to* ***1***. In dry box, 20 mg of $[K(2,2,2\text{-crypt})]_2[Ni_2Ge_9(PPh_3)]\cdot en$ crystals were dissolved in 4 ml DMF. ESI-MS data were recorded to confirm the presence of $[Ni_2Ge_9(PPh_3)]^-$ and $[K(2,2,2\text{-crypt})][Ni_2Ge_9(PPh_3)]^-$ ions before the interconversion experiment. The solution was placed in a Schlenk flask, the head gases evacuated and the flask back filled with CO gas. The reaction mixture was stirred for 3 h under the CO atmosphere. The resulting ESI-MS spectra showed decomposition of the starting material but did not show the formation of **1** or the $[Ni_2Ge_9(CO)]^-$ ion.

2.4. Crystallographic studies

2.4.1. $[K(2,2,2\text{-crypt})]_4[Ni_6Ge_{13}(CO)_5]\cdot 1.5en$ (1)

A black plate with approximate orthogonal dimensions $0.260\times0.196\times0.101\ mm^3$ was placed and optically centered on the Bruker SMART CCD system at −80 °C. The initial unit cell was indexed using a least-squares analysis of a random set of reflections collected from three series of 0.3° wide ω-scans. Data frames were collected [Mo Kα] with 0.2° wide ω-scans, 40 s per frame and 909 frames per series. Five data series were collected at varying ϕ angles ($\phi = 0°$, 72°, 144°, 216°, 288°), and finally, a partial repeat of the first series, 300 frames, for decay purposes. The crystal to detector distance was 4.903 cm, thus, providing a complete sphere of data to $2\theta_{max} = 55.0°$. A total of 96 582 reflections were collected and corrected for Lorentz and polarization effects and absorption using Blessing's method as incorporated into the program SADABS [21] with 27 463 unique ($R_{int} = 0.0330$).

System symmetry, lack of systematic absences and intensity statistics indicated the centrosymmetric triclinic space group $P\bar{1}$ (no. 2). The structure was determined by direct methods with the successful location of the heavy atom cluster and a few potassium atoms using the program XS [22]. The structure was refined with XL [22]. A multitude of least-squares difference-Fourier cycles were required to locate the remaining non-hydrogen atoms. All non-hydrogen, full occupancy, atoms were refined anisotropically. All of the hydrogen atoms were placed in calculated positions. Various disorders were found for the potassium crypt-and cations and each was optimized independently. A full and half occupancy ethylenediamine molecules were located and also optimized. The final difference-Fourier map possessed several large peaks that were all near heavy atoms while the remainder of the map was featureless indicating that the structure is both correct and complete. An empirical correction for extinction was also attempted but found to be negative and therefore not applied.

2.4.2. $[K(2,2,2\text{-crypt})]_2[Ni_2Ge_9(PPh_3)]\cdot en$ (2)

A black block with approximate orthogonal dimensions $0.152\times0.139\times0.068\ mm^3$ was mounted as above and cooled −100 °C. The data collection was performed as described above. A total of 75 805 reflections were collected and corrected for Lorentz and polarization effects and absorption using Blessing's method as incorporated into the program SADABS with 17 295 unique ($R_{int} = 0.0615$).

The structure was solved and refined using the SHELXTL program package [22] as described above. An empirical correction for extinction was also attempted but found to be negative and therefore not applied. The final difference-Fourier map possessed several large peaks that were all near heavy atoms while the remainder of the map was featureless indicating that the structure is both correct and complete.

3. Results and discussion

K_4Ge_9 and $Ni(CO)_2(PPh_3)_2$ react in ethylenediamine (en) in the presence of 2,2,2-crypt to give two different products that depend on reaction conditions. At moderate temperatures (30 °C < T < 40 °C), the $[Ni_6Ge_{13}(CO)_5]^{4-}$ ion (**1**) formed as the $[K(2,2,2\text{-crypt})]^+$ salt in moderate yield. The $[K(2,2,2\text{- crypt})]^+$ salt of **1** forms small, thin dark brown crystals is air and moisture sensitive in solution and the solid state. The salt is highly soluble in DMF and CH_3CN and forms dark brown solutions. The 19-atom cluster has a fused biicosahedral capsule-like structure with 17 Ge/Ni vertices and 2 centered Ni atoms. The structure and properties of this cluster will be discussed in subsequent sections.

At higher temperatures ($T \sim 118$ °C), the same reaction yields the $[Ge_9Ni_2(PPh_3)]^{2-}$ ion (**2**) in moderate yields, which crystallizes as large, block-like dark brown crystals of the $[K(2,2,2\text{-crypt})]^+$ salt. The structure of the anion has 1 Ni and 9 Ge vertices with a centered Ni atom and will also be discussed in subsequent sections. Both complexes have been characterized by single-crystal X-ray diffraction, NMR spectroscopy (^{13}C and ^{31}P where appropriate), Energy dispersive X-ray analysis (EDX), electrospray ionization mass spectrometry (ESI-MS) and infrared spectroscopy. Both salts are highly soluble in DMF and CH_3CN and decompose upon exposure to air in the solid state or in solution.

A proposed scheme for the interconversion of anions **1** and **2** is illustrated in Scheme 1. The transformation involves the initial formation of the cluster anion $[Ni_6Ge_{13}(CO)_5]^{4-}$ (**1**) followed by an irreversible conversion to $[Ge_9Ni_2(PPh_3)]^{2-}$ (**2**). This conclusion is based on the following results and observations:

(i) The same Ni precursor, $Ni(CO)_2(PPh_3)_2$, is used in the synthesis of **1** and **2**. However, anion **1** is isolated from reactions conducted at relatively lower temperatures (35–40 °C) and short reaction times whereas the formation of **1** is favored at high temperatures and long reaction times.

(ii) Electrospray mass spectra of DMF solutions of **1** (see following section) show anion **1** as well as, $[Ge_9Ni_2(CO)]^-$ and $[Ge_9Ni_2]^-$, that result from fragmentation of the parent. These ions have the same Ge_9Ni_2 core composition of **2**.

(iii) Addition of PPh_3 to en solutions of pure $[K(2,2,2\text{-crypt})]_4[Ni_6Ge_{13}(CO)_5]$ results in the formation of **2** after ~30 min of reaction at 118 °C. The ESI-MS spectra of these solutions show signals

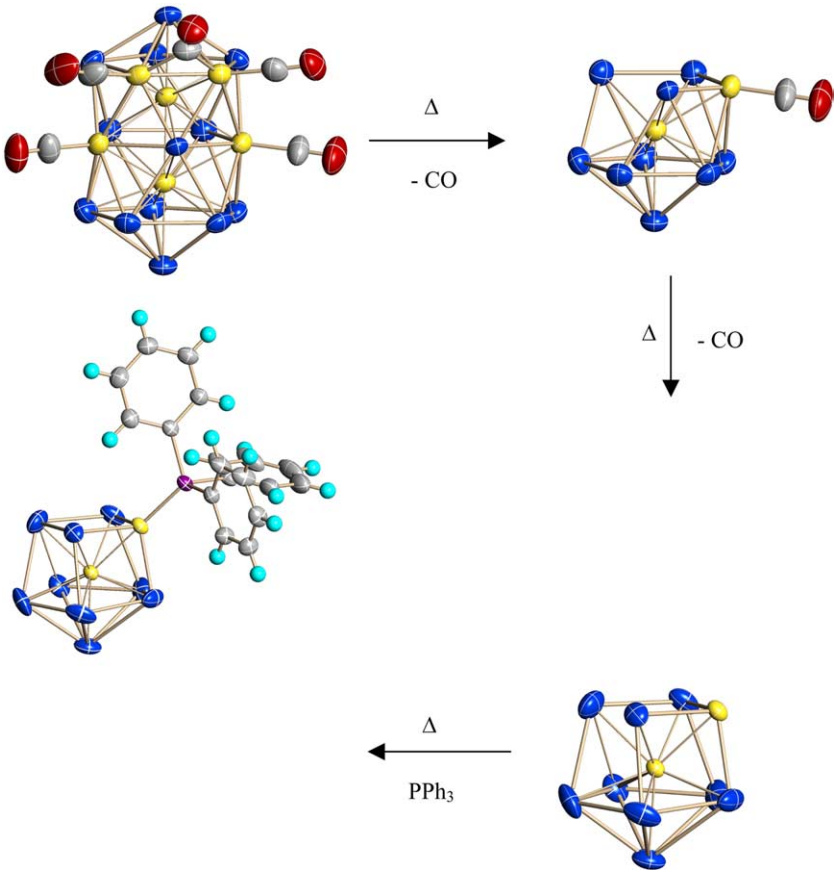

Scheme 1.

corresponding to $K[Ge_9Ni_2(PPh_3)]^{1-}$ and $[Ge_9Ni_2(PPh_3)]^{1-}$ ions, that coincide with those of the authentic sample.

(iv) Reactions between **2** and carbon monoxide result in cluster decomposition but do not regenerate **1** or result in the formation of $[Ge_9Ni_2(CO)]^-$ according to ESI-MS analysis.

While these experiments show that **2** can be generated from **1** under appropriate conditions, they do not preclude the direct formation of **2** from Ge_9^{4-} and $Ni(CO)_2(PPh_3)_2$.

Indeed, the synthesis of closely related clusters such as $[Sn_9Pt_2(PPh_3)]^{2-}$ appear to form directly from Sn_9^{4-} with sequential addition of Pt fragments (NMR analysis) [15] and do not seem to involve intermediates akin to **1**. Moreover, the proposed mechanism for the formation of the closely related $[Ni_3@Ge_{18}]^{4-}$ involves direct insertion of Ni into a Ge_9 cluster and a subsequent coupling [13].

3.1. Mass spectrometry

The electrospray mass spectrum for each sample was recorded in the negative ion mode from DMF solutions of crystalline $[K(2,2,2\text{-crypt})]^+$ salts. The distinctive mass envelopes arising from the multiple isotopes of Ge and Ni have been simulated to facilitate assignments and verify nuclearities. The spectrum for $K[Ge_9Ni_2(PPh_3)]^{1-}$ is shown in Fig. 1 as an example and the remaining spectra and simulations are given in the Supporting Information. The spectrum of **1** (Fig. S1) shows weak signals of the [K(2,2,2-crypt)]-coordinated molecular ion of $[Ni_6Ge_{13}(CO)_5]^-$ along with the decarbonyl loss products $Ni_6Ge_{13}(CO)_4^-$, $Ni_6Ge_{13}(CO)_2^-$ and ligand-free binary ion $Ni_6Ge_{13}^-$. Patterns of new compounds, $Ge_9Ni_2(CO)^-$ and $Ge_9Ni_2^-$ are also observed as well as peaks for the $Ge_4Ni_4(CO)_4^-$ cluster ion paired to K^+ and $[K(2,2,2\text{-crypt})]^+$.

The negative ion electrospray mass spectrum of DMF solution constituted from crystalline $[K(2,2,2\text{-crypt})]_2[Ge_9Ni_2(PPh_3)]$ shows an intense signal for the $K[Ge_9Ni_2(PPh_3)]^{1-}$ molecular ion with the expected mass envelope (Fig. 1). As is common for these types of Zintl ions, the potassium-coordinated ion pair, $K[Ge_9Ni_2(PPh_3)]^{1-}$, appears as the parent ion, (m/z 1072.1) and the fully charged anion is not observed. The ligand-free Ge–Ni cluster anion $K[Ge_9Ni_2]^{1-}$ was also observed as well as the CO substituted cluster, $K[Ge_9Ni_2(CO)]^{1-}$, which presumably results from a trace contamination in the sample.

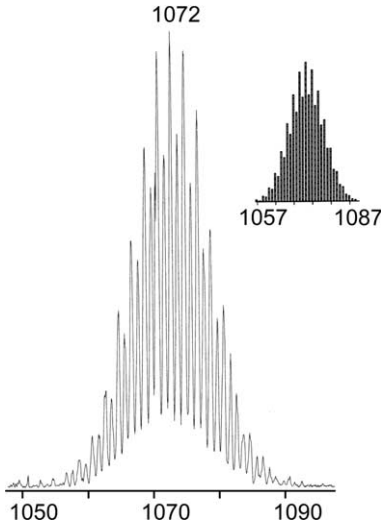

Fig. 1. ESI-mass spectrum of the $K[Ge_9Ni_2(PPh_3)]^{1-}$ molecular ion. The inset shows the simulated mass envelope.

3.2. Solid-state structures

The $[Ni_6Ge_{13}(CO)_5]^{4-}$ (**1**) and $[Ge_9Ni_2(PPh_3)]^{2-}$ (**2**) anions crystallize as the $[K(2,2,2\text{-crypt})]^{+}$ salts with triclinic crystal symmetry, space group $P\bar{1}$. The former has 1.5en solvate molecules per formula unit. A summary of the crystal data is given in Table 1, and selected bond distances are given in Tables 2 and 3, respectively. A previous report of the $[K(2,2,2\text{-crypt})]_2[Ge_9Ni_2(PPh_3)]$ structure was incorrectly characterized as having an anion formula $[Ge_{10}Ni(PPh_3)]^{2-}$. We correct this interpretation here and present a new refinement of the crystal structure from new X-ray data.

The $[Ni_6Ge_{13}(CO)_5]^{4-}$ anion possesses C_s point symmetry with a symmetry plane defined by Ge1, Ge8, Ge19 and the bridging carbonyl (Fig. 2). The anion is a 17-vertex deltahedral cluster defined by 13 Ge atoms and 4 Ni atoms. The cluster is centered by two additional interstitial Ni atoms. Each of the 4 vertex Ni atoms has a terminal CO ligand bound in a radial fashion with an additional bridging CO spanning the Ni2–Ni3 edge. The 17-atom deltahedron possesses 126 total valence electrons and has 32 cluster electrons according to Wades rules of electron counting [14]. According to Wades Rules, each of the Ge atoms contributes 2 electrons whereas each Ni(CO) vertex unit and interstitial Ni contributes zero electrons. The bridging CO ligand and the cluster charge contribute 2 and 4 electrons, respectively, to give 32 cluster electrons

$$13 \times 2(\text{Ge}) + 2(\text{CO}) + 4(\text{charge}) = 32\text{e}.$$

The 17-vertex, 32 electron cluster corresponds to a hypo-*closo* electron count and is consistent with the closed, deltahedral structure type.

The $[Ni_6Ge_{13}(CO)_5]^{4-}$ structure can be viewed as two interpenetrating icosahedral units (**Ih1** and **Ih2**) that share the central $Ge_3Ni_2(CO)_2$ penagonal ring and the 2 interstitial Ni atoms of the biicosahedral cluster (see Fig. 2(b)). **Ih1** has a composition $Ge_7Ni_6(CO)_5$ where Ni7 is interstitial and Ni13 occupies a vertex. **Ih2** has a $Ge_9Ni_4(CO)_2$ composition where Ni7 occupies a vertex and Ni13 occupies the interstitial site. This type of interpenetrating biicosahedral structure is new for transition metal Zintl clusters but is known in some of Teo's bimetallic Au–Ag and trimetallic Au–Ag–M; M = Pt, Pd, Ni supraclusters. In particular, the structure of **1** is highly

Table 1
Summary of crystallographic data for the $[Ni_6Ge_{13}(CO)_5]^{4-}$ and $[Ge_9Ni_2(PPh_3)]^{2-}$ ions

Empirical formula	$[K(2,2,2\text{-crypt})]_2[\mathbf{2}]\cdot$ en	$[K(2,2,2\text{-crypt})]_4[\mathbf{1}]\cdot 1.5$en
Compound formula	$C_{78.5}H_{150}Ge_{13}K_4N_{9.5}Ni_6O_{29}$	$C_{56}H_{95}Ge_9K_2N_6Ni_2O_{12}P$
Formula weight	3143.41	1924.28
Temperature (K)	193(2)	173(2)
Wavelength (Å)	0.71073	0.71073
Crystal system	triclinic	triclinic
Space group	$P\bar{1}$	$P\bar{1}$
a (Å)	15.2287(4)	12.9083(11)
b (Å)	16.1988(4)	13.0373(11)
c (Å)	26.1824(7)	23.569(2)
α (°)	92.7560(10)	96.546(2)
β (°)	91.3490(10)	104.757(2)
γ (°)	11.2730(10)	96.868(2)
Volume (Å^3)	6006.0(3)	3764.7(6)
Z	2	2
D_{calc} (g/cm^3)	1.738	1.698
Absolute coefficient (mm^{-1})	4.319	4.212
Data/restraints/parameters	27463/2340/1437	17295/5/790
Goodness-of-fit on F^2	1.118	1.029
Final R indices $[I > 2\sigma(I)]$[a]	$R_1 = 0.0549$; $wR_2 = 0.1794$	$R_1 = 0.0428$; $wR_2 = 0.1007$
R indices (all data)[a]	$R_1 = 0.0839$; $wR_2 = 0.1936$	$R_1 = 0.0834$; $wR_2 = 0.1111$

[a] The function minimized during the full-matrix least-squares refinement was $\sum w(F_o^2 - F_c^2)$ where $w = 1/[\sigma^2(F_o^2) + (0.050 * P)^2 + 1.3423 * P]$ and $P = \max(F_o^2, 0) + 2 * F_c^2)/3$.

Table 2
Selected bond distances (Å) and angles (°) for the $[Ge_{13}Ni_6(CO)_5]^{4-}$ ion

Ge(1)–Ni(2)	2.668(1)
Ge(1)–Ni(7)	2.474(1)
Ge(4)–Ni(3)	2.610(1)
Ge(4)–Ni(7)	2.438(1)
Ge(4)–Ni(9)	2.557(1)
Ge(5)–Ni(7)	2.431(1)
Ge(8)–Ni(2)	2.508(1)
Ge(8)–Ni(7)	2.381(1)
Ge(1)–Ge(4)	2.658(1)
Ge(1)–Ge(5)	2.906(1)
Ge(4)–Ge(5)	2.892(1)
Ge(4)–Ge(10)	2.735(1)
Ge(5)–Ge(10)	2.659(1)
Ge(5)–Ge(11)	2.706(1)
Ge(8)–Ge(15)	2.703(1)
Ge(10)–Ge(11)	2.862(1)
Ni(2)–Ni(7)	2.606(1)
Ni(2)–Ni(12)	2.742(1)
Ni(3)–Ni(9)	2.771(1)
Ni(7)–Ni(13)	2.564(1)
Ni(7)–Ni(9)	2.637(1)
Ni(9)–Ni(13)	2.610(1)
Ge(8)–Ni(9)	2.497(1)
Ge(10)–Ni(7)	2.522(1)
Ge(10)–Ni(9)	2.574(1)
Ge(10)–Ni(13)	2.595(1)
Ge(14)–Ni(12)	2.666(1)
Ge(14)–Ni(13)	2.575(1)
Ge(15)–Ni(9)	2.605(1)
Ge(16)–Ni(13)	2.499(1)
Ge(10)–Ge(16)	2.638(1)
Ge(10)–Ge(17)	2.820(1)
Ge(14)–Ge(15)	2.749(1)
Ge(14)–Ge(19)	2.741(1)
Ge(15)–Ge(16)	2.675(1)
Ge(16)–Ge(17)	2.777(1)
Ge(16)–Ge(19)	2.808(1)
Ge(17)–Ge(19)	2.772(1)
Ni(2)–C(2)	1.694(8)
Ni(2)–C(23′)	1.859(8)
Ni(3)–C(3)	1.712(8)
Ni(3)–C(23′)	1.898(8)
Ni(9)–C(9)	1.715(8)
Ni(12)–C(12)	1.750(8)
Ni(2)–Ge(1)–Ni(3)	54.80(3)
Ge(4)–Ge(1)–Ge(5)	62.44(3)
Ge(4)–Ge(5)–Ge(6)	97.67(3)
Ge(1)–Ni(7)–Ni(13)	173.03(4)
Ge(5)–Ni(7)–Ge(8)	173.04(4)
Ge(6)–Ni(7)–Ni(9)	169.49(4)
Ge(4)–Ni(9)–Ge(16)	122.46(4)
Ge(6)–Ge(11)–Ge(17)	157.25(4)
Ge(8)–Ni(13)–Ge(15)	65.11(3)
Ge(16)–Ni(13)–Ni(12)	171.06(4)
Ge(19)–Ni(13)–Ni(7)	176.55(4)
Ge(16)–Ni(17)–Ge(18)	106.81(3)
C(23′)–Ni(2)–Ge(6)	140.70(2)
C(3)–Ni3–C(23)	106.10(4)
C(9)–Ni(9)–Ge(8)	127.50(3)
Ni(3)–C(23′)–Ni(2)	81.40(2)

Table 3
Selected bond distances (Å) and angles (°) for the $[Ge_9Ni_2(PPh_3)]^{2-}$ ion

Ni(1)–P(1)	2.121(1)
Ge(1)–Ni(1)	2.381(1)
Ge(3)–Ni(1)	2.371(1)
Ge(9)–Ni(1)	2.370(1)
Ni(1)–Ni(2)	2.359(1)
Ge(1)–Ni(2)	2.350(1)
Ge(2)–Ni(2)	2.433(1)
Ge(3)–Ni(2)	2.368(1)
P(1)–C(1)	1.847(4)
P(1)–C(2)	1.843(4)
P(1)–C(3)	1.840(4)
Ge(1)–Ge(2)	2.640(1)
Ge(1)–Ge(8)	2.608(1)
Ge(2)–Ge(3)	2.634(1)
Ge(2)–Ge(5)	2.722(1)
Ge(2)–Ge(6)	2.733(1)
Ge(3)–Ge(4)	2.594(1)
Ge(4)–Ge(9)	2.633(1)
Ge(4)–Ge(7)	2.692(1)
Ge(4)–Ge(5)	2.788(1)
Ge(5)–Ge(7)	2.642(1)
Ge(5)–Ge(6)	2.656(1)
Ge(6)–Ge(7)	2.657(1)
Ge(6)–Ge(8)	2.808(1)
Ge(7)–Ge(8)	2.692(1)
Ge(8)–Ge(9)	2.635(1)
Ni(2)–Ge(1)–Ni(1)	59.82(2)
Ni(1)–Ge(1)–Ge(8)	92.35(3)
Ni(1)–Ge(1)–Ge(2)	82.29(2)
Ge(8)–Ge(1)–Ge(2)	108.20(2)
Ni(2)–Ge(2)–Ge(3)	55.56(2)
Ge(3)–Ge(2)–Ge(1)	89.45(2)
Ge(3)–Ge(2)–Ge(5)	68.03(2)
Ge(1)–Ge(2)–Ge(5)	107.92(2)
Ni(2)–Ge(4)–Ge(3)	56.16(2)
Ge(3)–Ge(4)–Ge(9)	82.94(2)
Ge(9)–Ge(4)–Ge(7)	76.38(2)
Ge(9)–Ge(4)–Ge(5)	109.40(2)
Ge(7)–Ge(4)–Ge(5)	57.60(2)
Ge(9)–Ni(2)–Ge(1)	94.80(3)
Ge(1)–Ni(2)–Ni(1)	60.75(2)
Ge(1)–Ni(2)–Ge(3)	103.73(3)
Ge(1)–Ni(2)–Ge(7)	128.30(3)
Ni(1)–Ni(2)–Ge(7)	148.06(3)
Ge(3)–Ni(2)–Ge(8)	157.16(3)
Ni(2)–Ni(1)–Ge(3)	60.08(2)
P(1)–Ni(1)–Ni(2)	177.23(4)
P(1)–Ni(1)–Ge(9)	122.79(4)
P(1)–Ni(1)–Ge(3)	117.45(4)
C(1)–P(1)–Ni(1)	119.34(1)
C(2)–P(1)–Ni(1)	112.37(1)
C(2)–P(1)–C(1)	100.69(2)
C(3)–P(1)–C(2)	102.21(2)
C(3)–P(1)–C(1)	117.79(1)

reminiscent of the *sss* rotamer of the $[(PPh_3)_{10}Au_{13}Ag_{12}Br_8]^+$ triicosahedral cluster [20].

The Ge–Ge, Ni–Ni, and Ni–Ge bond distances are in the range of 2.658(1)–2.894(1) Å (avg. 2.746(4) Å), 2.450(1)–2.771(1) Å (avg. 2.624(4) Å), and 2.381(1)–2.668(1) Å (avg. 2.522(5) Å), respectively (see Table 2). As expected, $Ni–CO_{(terminal)}$ contacts (avg. 1.718(8) Å) are shorter than the $Ni–CO_{(bridge)}$ contacts (avg. 1.879(8) Å). The structure is slightly flattened along the Ge8–Ge14 and Ge8–Ge5 vectors. This distortion is best illustrated by the differences between the 6 diagonal distances in each icosahedral subunit. In both of the icosahedral cages, diagonal distances involving Ge8, (Ge8–

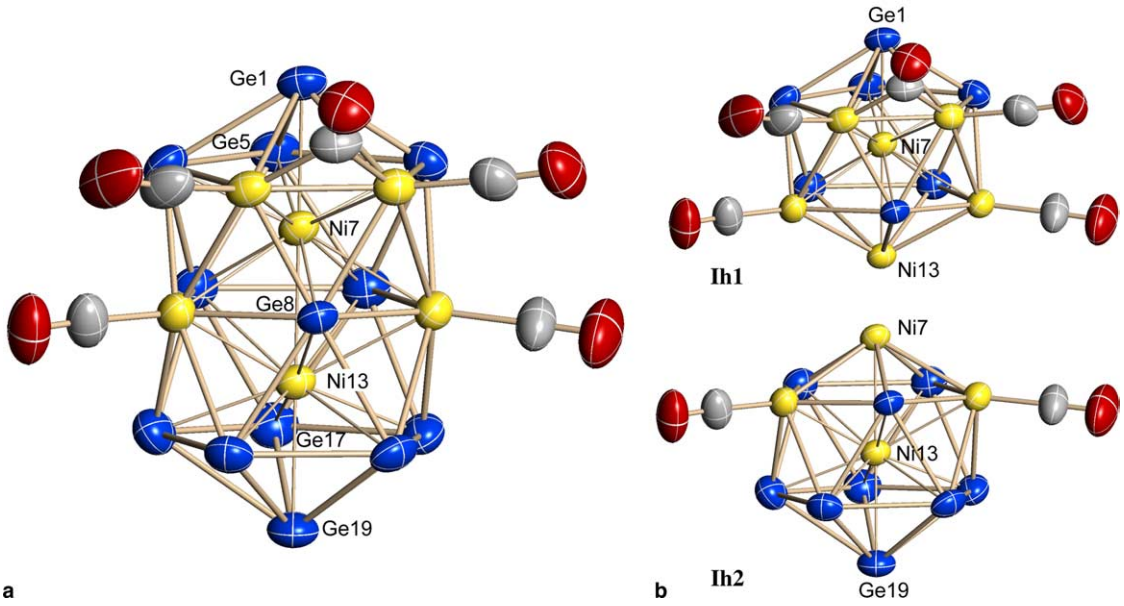

Fig. 2. (a) ORTEP drawing of the $[Ni_6Ge_{13}(CO)_5]^{4-}$ anion. Ni is yellow, Ge is blue, C is gray and oxygen is red. A fully labeled drawing is given in the Supporting material. (b) The two interpenetrating icosahedral subunits, Ih1 and Ih2.

Ge5 = 4.812(1) Å for **Ih1**, and Ge8–Ge17 = 4.878(2) Å for **Ih2**) are shorter than the other 5 diagonals in the respective subunits (5.087(5) Å, avg. for **Ih1**, and 5.115(4) Å avg. for **Ih2**).

The Ge–Ge bond distances for the anion **1** (2.6335(9)–2.9064(11); 2.750(6) Å avg.) are similar to those in other polygermenide clusters such as $[K(2,2,2\text{-crypt})]_3[P(C_6H_5)_3Ge_9]$, where Ge–Ge distances vary from 2.53 to 3.27 Å [23–25]. The Ni–Ge (2.3808(9)–2.6681(11) Å; 2.523(5) Å av.) and Ni–Ni (2.450(1)–2.771(1) Å, 2.624(4) Å av.) contacts are similar to the reported compounds (2.470–2.691 and 2.553–2.721 Å, respectively) [26].

As mentioned previously, the structure of the $[Ge_9Ni_2(PPh_3)]^{2-}$ ion, (**2**), was incorrectly reported to have the formula $[Ge_{10}Ni(PPh_3)]^{2-}$ in which the interstitial atom was refined as Ge. The formula has been unequivocally established by ESI-MS studies and the structure re-determined. The structure (Fig. 3) is identical to that previously reported except for the identity of the centered atom. The anion has virtual C_{3v} point symmetry and is isoelectronic and isostructural to $[Sn_9Pt_2(PPh_3)]^{2-}$ [15]. It is defined by nine surface Ge atoms, one interstitial Ni atom and a capping $[Ni(PPh_3)]$ fragment. The cluster is a 10-vertex 20-electron hypo-*closo* system that has an open, *nido*-like structure. For comparison, it is isostructural to the 24-electron 10-vertex $[Sb_7Ni_3(CO)_3]^{3-}$ ion that adopts a *nido*-type architecture [27]. Note that replacing the centered Ni atom with a Ge atom would add 4 electrons to cluster bonding and would be consistent with the observed structure. Although this does not occur, this

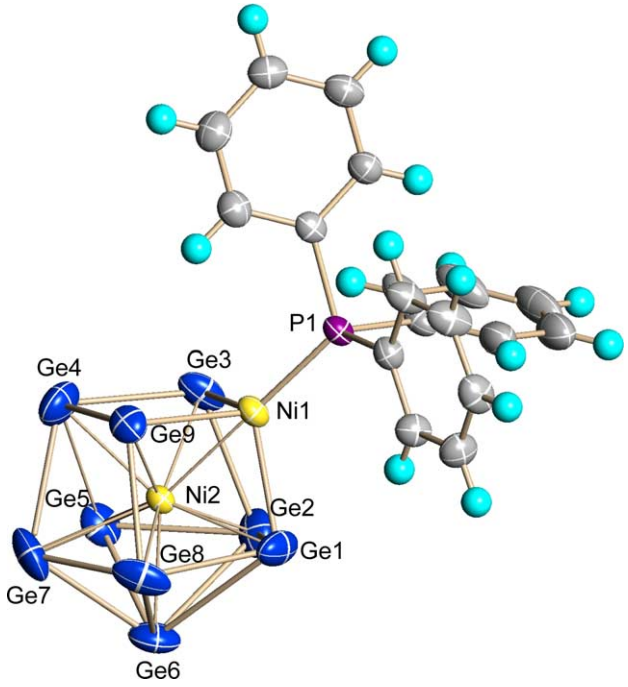

Fig. 3. ORTEP drawing of the $[Ge_9Ni_2(PPh_3)]^{2-}$ ion, (**2**). Ni is yellow, Ge is blue, C is gray, P is purple and H is turquoise.

electron counting rationale gave rise to the erroneous assignment in the original publication [18].

The centered Ni atom has nine Ni–Ge contacts in the range of 2.342(6)–2.447(6) Å. The 3 Ni–Ge bonds to Ni1 average 2.37(2) Å. The Ge–Ge contacts are in the range 2.594(1)–2.808(1) Å and are typical of polygerminide cages.

3.3. NMR spectroscopic studies

The ^{13}C NMR spectrum of $[Ni_6Ge_{13}(CO)_5]^{4-}$ (DMSO-d_6, 25 °C) shows carbonyl resonances at 194.6, 217.9, 224.9 ppm, which is consistent with the solid state structure.

The room temperature ^{31}P NMR spectrum of $[Ge_9Ni_2(PPh_3)]^{2-}$ crystals shows only free triphenylphosphine in DMF solution ($\delta = -5.1$ ppm), suggesting that PPh_3 ligand dissociation is fast on the NMR time scale. This observation is somewhat surprising in view of the static nature of the PPh_3 ligand in the isoelectronic, isostructural $[Sn_9Pt_2(PPh_3)]^{2-}$ ion and the electron deficient nature of the cluster.

4. Conclusions

In our original report, the centered atom of **2** was modeled as both Ni and Ge with ultimate selection of the latter. Due to the similarities in the scattering factors of Ni and Ge, the refinement of the X-ray data did not allow for the discrimination between the two models. The assignment of a centered Ge atom was primarily based on electron counting principles (Wades rules) and striking structural similarities to other clusters of the same nuclearity (e.g., $[Sb_7Ni_3(CO)_3]^{3-}$). With the discovery of $[Sn_9Pt_2(PPh_3)]^{2-}$, we were prompted to reinvestigate the Ni–Ge system and the identity of **2**. The higher precision CCD data reported here and, more importantly, the ESI-MS data unequivocally identify the ion as $[Ge_9Ni_2(PPh_3)]^{2-}$ with a centered Ni atom. The non-deltahedral *nido*-like structures of these hypo-*closo* clusters are presumably due to steric demands of the centered metal atom.

During our re-investigation of the synthesis of **2**, we found that the $[Ni_6Ge_{13}(CO)_5]^{4-}$ ion, **1**, was formed at lower temperatures and shorter reaction times. While we have shown that **2** can be formed from **1** (Scheme 1), it seems quite possible that it also forms directly from Ge_9^{4-} and the $Ni(CO)_2(PPh_3)_2$. The biicosahedral structure of **1** is unique to Zintl ion chemistry but is a known feature in bimetallic clusters of the coinage metals [20]. The recently reported $[Pd_2@Ge_{18}]^{4-}$ and $[Ni_3@(Ge_9)_2]^{4-}$ cluster anions also in this general class of compounds. The former is an 18 vertex, 2 focus, 40 electron cluster with the expected *closo* architecture ($2n + 2$ cluster electrons per focus) whereas the latter does not easily fit into a Wadian description. Interestingly, neither forms icosahedral structures and are structurally distinct from **1**.

Recently, we have shown that ligand-free deltahedral clusters of Pb and Sn that are compositionally similar to the ligand-free ions identified here. For example, $[Ni@Pb_{10}]^{2-}$ and the gas phase $[Ni@Pb_{10}]^{1-}$ ions are centered 10-vertex clusters [10] similar to $Ge_9Ni_2^{-1}$ (or $[Ni@Ge_9Ni]^{-1}$). The later presumably adopts the *nido*-like C_{3v} structure of **2** despite having *5 fewer electrons* than the 22-electron *closo*-$[Ni@Pb_{10}]^{2-}$ cluster. While many of Zintl clusters of the group 14 elements and their transition metal derivatives adopt Wadian like structures, there are now several examples that do not. It is certain that more exceptions will be discovered as research continues.

Acknowledgments

We dedicate this manuscript to Professor Malcolm Chisholm on the occasion of his 60th birthday. This material is based upon work supported by the National Science Foundation under Grant No. 0401850.

Appendix A. Supplementary data

Crystallographic data for the compounds have been deposited with the Cambridge Crystallographic Data Centre, CCDC Nos. 273776 (**1**) and 273777 (**2**). Copies of this information may be obtained free of charge from The Director, CCDC, 12 Union Road, Cambridge, CB2 1EZ, UK (fax: +44 1223 3360333 or e-mail: deposit@ccdc.cam.ac.uk or http://www.ccdc.cam.ac.uk). Supplementary data associated with this article can be found, in the online version, at doi:10.1016/j.poly.2005.07.031.

References

[1] T.F. Fassler, S.D. Hoffmann, Angew. Chem. Int. Ed. 43 (2004) 6242.
[2] L. Yong, S.D. Hoffmann, T.F. Fassler, Z. Anorg. Allg. Chem. 630 (2004) 1977.
[3] T.F. Fassler, Angew. Chem. Int. Ed. 40 (2001) 4161.
[4] J.M. Goicoechea, S.C. Sevov, Inorg. Chem. 44 (2005) 2654.
[5] S. Neukermans, E. Janssens, Z.F. Chen, R.E. Silverans, P.V. Schleyer, P. Lievens, Phys. Rev. Lett. 92 (2004).
[6] R.B. King, T. Heine, C. Corminboeuf, P.V. Schleyer, J. Am. Chem. Soc. 126 (2004) 430.
[7] M.J. Moses, J.C. Fettinger, B.W. Eichhorn, Science 300 (2003) 778.
[8] R.C. Haushalter, C.M. O'Connor, J.P. Haushalter, A.M. Umarji, G.K. Shenoy, Angew. Chem. Int. Ed. 23 (1984) 169.
[9] E.N. Esenturk, B. Eichhorn, J. Fettinger (to be published).
[10] E.N. Esenturk, J. Fettinger, B. Eichhorn, Chem. Commun. (2005) 247.
[11] E.N. Esenturk, J. Fettinger, Y.F. Lam, B. Eichhorn, Angew. Chem. Int. Ed. 43 (2004) 2132.
[12] J.M. Goicoechea, S.C. Sevov, J. Am. Chem. Soc. 127 (2005) 7676.
[13] J.M. Goicoechea, S.C. Sevov, Angew. Chem. Int. Ed. 44 (2005) 4026.
[14] K.J. Wade, Adv. Inorg. Chem. Radiochem. 18 (1976) 1.
[15] B. Kesanli, J. Fettinger, D.R. Gardner, B. Eichhorn, J. Am. Chem. Soc. 124 (2002) 4779.
[16] S. Lee, Inorg. Chem. 31 (1992) 3063.

[17] B. Kesanli, J.C. Fettinger, D.R. Gardner, B.W. Eichhorn, Chem. Eur. J. (2001) 5277.
[18] D.R. Gardner, B.W. Eichhorn, J. Fettinger, Angew. Chem. Int., Ed. Engl. 35 (1996) 2852.
[19] B.K. Teo, H. Zhang, Y. Kean, H. Dang, X.B. Shi, J. Chem. Phys. 99 (1993) 2929.
[20] B.K. Teo, H. Zhang, Coord. Chem. Rev. 143 (1995) 611.
[21] G.M. Sheldrick, Universitat Gottingen, Gottingen, Germany, 1996.
[22] G.M. Sheldrick, Siemens Analytical X-ray Instruments, Inc., Madison, WI, 1994.
[23] C. Belin, H. Mercier, V. Angilella, New J. Chem. 15 (1991) 931.
[24] L. Yong, S.D. Hoffmann, T.F. Fassler, Z. Anorg. Allg. Chem. 631 (2005) 1149.
[25] C. Downie, Z.J. Tang, A.M. Guloy, Angew. Chem. Int. Ed. 39 (2000) 338.
[26] A. Ceriotti, F. Demartin, B.T. Heaton, P. Ingallina, G. Longoni, M. Manassero, M. Marchionna, N. Masciocchi, J. Chem. Soc., Chem. Commum. (1989) 786.
[27] S. Charles, B.W. Eichhorn, S.G. Bott, J. Am. Chem. Soc. 115 (1993) 5837.